Sanjeev Sharma[1], Kajol Maheshwari[1]

ELASTIC-PLASTIC TRANSITION IN FUNCTIONALLY GRADED THIN ROTATING ORTHOTROPIC DISK WITH VARIABLE THICKNESS AND DENSITY

ELASTOPLASTIČNI PRELAZNI NAPONI U TANKOM ROTIRAJUĆEM ORTOTROPNOM DISKU PROMENLJIVE DEBLJINE I GUSTINE OD FUNKCIONALNOG KOMPOZITA

Originalni naučni rad / Original scientific paper
UDK /UDC: 66:539.319

Rad primljen / Paper received: 5.06.2019

Adresa autora / Author's address:
[1)] Department of Mathematics, Jaypee Institute of Information Technology, Noida, India
email: sanjeev.sharma@jiit.ac.in ; kajolm.maths@gmail.com

Keywords
- elastic, plastic
- functionally graded material
- orthotropic material
- thickness
- density
- rotating disk

Abstract

Transitional and fully plastic stresses for a thin rotating disk made up of functionally graded material with variable thickness and density have been investigated in this paper using the transition theory which eliminates the assumption of yield condition. Analytical expressions for angular speed and circumferential stresses at initial yielding and fully plastic state have been obtained. From the numerical discussion on angular speed and circumferential stresses, it has been analysed that rotating disk made up of functionally graded isotropic material (steel) is a better choice for engineering design as compared to functionally graded orthotropic disk (barite and topaz) because disk of isotropic material has less circumferential stress than that of orthotropic material.

Ključne reči
- elastičan, plastičan
- funkcionalni kompozitni materijal
- ortotropni materijal
- debljina
- gustina
- rotirajući disk

Izvod

U radu su istraženi prelazni i potpuno plastični naponi kod tankog rotirajućeg diska promenljive debljine i gustine od funkcionalnog kompozita, primenom prelazne teorije napona, kojom se eliminiše pretpostavka stanja tečenja. Dobijeni su analitički izrazi ugaone brzine i obimskih napona pri inicijalnom tečenju i stanju potpune plastičnosti. Diskusija numeričkog proračuna o ugaonoj brzini i obimskim naponima daje analizu prema kojoj je disk od izotropnog funkcionalnog materijala (čelik) bolji izbor u projektovanju konstrukcija, u poređenju sa diskom od ortotropnog funkcionalnog materijala (barit i topaz), jer su obimski naponi manji kod diska od izotropnog materijala u odnosu na ortotropni materijal.

INTRODUCTION

Rotation of a circular disk plays a vital role in many engineering designs like rotors, compressors, flywheel, turbines, computer disc drives, etc. Analysing elastic-plastic stresses in rotating disks is an important part of solid mechanics which has been discussed by Timoshenko et al. /1/, Sadd /2/ and Chakrabarty /3/. Functionally graded materials, also known as non-homogeneous composite materials with varying composition and are widely used in engineering areas and aerospace industry. Suresh et al. /4/ discussed the fundamentals of the materials that are functionally graded. Von-Mises yield criterion and swift hardening law have been used to derive the plastic stresses for annular disk by Eraslan et al. /5/. Numerical investigation of elastic-plastic stresses in rotating disk has been done by You et al. /6/ using polynomial based stress-strain relation. Radaković et al. /7/ evaluate the ductile crack growth using potential drop and magnetic emission signals. Finite difference method has been used to obtain thermal stresses and strains for rotating disk with variable thickness and density by Sharma et al. /8/ and found that rotating disk of functionally graded material has less circumferential stress. Analytic and semi-analytic solutions have been obtained by Bayat et al. /9/ for rotating disk having hyperbolic convergent or parabolic thickness profile and concluded that the rotating disk with parabolic concave profile is better for engineering design. The change in location of maximum von-Mises stress has been investigated for functionally graded rotating disks with non-uniform thickness and variable angular velocity by Zheng et al. /10/ using finite difference method. Thermal elastic stresses under the effect of magnetic field in a functionally graded rotating disk have been determined by Dai et al. /11/ using semi-analytic approach and they discussed the influence of different material parameters on functionally graded rotating disk. Semi-analytical solutions based on deformation theory for rotating disk have been presented by Bayat et al. /12/ and they investigated the influence of material grading index and disk geometry for stress and displacement field. Bahaloo et al. /13/ observed that critical speed which decreases the performance of disk has been reduced in a functionally graded annular disk with a circumferential crack inside and outside of the plane. By generalizing the plane stress solution from two-dimensional to three-dimensional, Ahsgari et al. /14/ determined stresses for thick and hollow functionally graded rotating disks. Bayat et al. /15/ considered a rotating functionally graded disk with variable thickness under steady state temperature and found that stresses with convergent profile are smaller than that with uniform thickness, while weight of disk with

concave profile is least. Çallıoğlu et al. /15/ investigated the stresses for the functionally graded disk and concluded that analytical and numerical solutions are approximately the same. Dai et al. /17/ evaluated the stresses in a hollow rotating functionally graded disk with angular acceleration under the effect of temperature field using semi-analytical approach. Remarkable nonlinear behaviour has been observed by Zafarmand et al. /18/ for high angular velocities in functionally graded thick rotating disks made up of nanocomposites. The creep behaviour of isotropic rotating disk with thermal gradient has been determined by Bose et al. /19/ using von-Mises yield criterion and have examined the impact of temperature change on strain rates and creep behaviour of the rotating disk.

Semi empirical laws and yield criterions i.e. Tresca, von-Mises yield criterions etc. have been used by above authors. Our approach starts from eliminating the necessity of yield condition and semi-empirical laws etc., by considering transition region as an asymptotic region from elastic to plastic state or elastic to creep state. Borah /20/ discussed the transition theory with an example of shell under uniform pressure and steady state temperature and derived the transition and plastic stresses. Stresses have been obtained by Sharma et al. /21/ using transition theory for a functionally graded orthotropic non-homogeneous hollow cylinder and concluded that the cylinder of isotropic material has higher circumferential stresses than that of orthotropic material. Further, Sharma /22/ evaluated the fully plastic stresses for functionally graded circular cylinder with thermal effect using transition theory and found that the thermal effect gives better result for functionally graded cylinder. Plastic stresses for transversely isotropic thick-walled cylinder have been obtained by Sharma et al. /23/ using generalized strain measure and observed that isotropic material is a better option for circular cylinder with thermal effect than that of transversely isotropic cylinder. Sharma et al. /24/ evaluated creep stresses for thin rotating disk made up of functionally graded orthotropic material and concluded that the material with high functionally graded property is a better option for design.

In this paper, we have evaluated transitional and plastic stresses for a functionally graded thin orthotropic rotating disk using transition theory. The objective of the problem is to evaluate the angular speed, transitional and fully plastic stresses for functionally graded thin orthotropic rotating disk with variable thickness and density using the transition theory which helps in eliminating the assumption of semi-empirical laws.

BASIC EQUATIONS OF THE PROBLEM

Consider a thin rotating disk made of functionally graded material whose thickness and density varies radially. The internal radius of the thin circular disk is considered to be a and external radius is b. The displacement components for the circular disk with co-ordinates in the cylindrical polar system are considered to be

$$X = r(1-\beta),\ Y = 0 \text{ and } Z = \alpha z \tag{1}$$

where: $\beta = \beta(r)$ and α is a constant.

The strain measure /20/ in generalized form is

$$e_{ii} = \frac{1}{n}\left[1-(1-2e_{ii}^{A})^{n/2}\right],\ \ (i=1,2,3),$$

where: n is nonlinear measure; and e_{ii}^{A} be finite components of principal strain.

Using the above strain measure, we get

$$e_{rr} = \frac{1-(r\beta'+\beta)^n}{n},\ e_{\theta\theta} = \frac{1-\beta^n}{n},\ e_{zz} = \frac{1-(1-\alpha)^n}{n}, \tag{2}$$

where: $\beta' = d\beta/dr$ and all other strain components are zero.

The stress components for the orthotropic materials are given as

$$\begin{aligned} T_{rr} &= S_{11}[1-(r\beta'+\beta)^n]+S_{12}[1-\beta^n]+S_{13}[1-(1-\alpha)^n],\\ T_{\theta\theta} &= S_{21}[1-(r\beta'+\beta)^n]+S_{22}[1-\beta^n]+S_{23}[1-(1-\alpha)^n], \\ T_{zz} &= 0. \end{aligned} \tag{3}$$

Considering the non-homogeneity in orthotropic material as

$$S_{11} = \frac{S_{011}}{n}\left(\frac{r}{b}\right)^{-p},\ S_{12} = \frac{S_{012}}{n}\left(\frac{r}{b}\right)^{-p},\ S_{13} = \frac{S_{013}}{n}\left(\frac{r}{b}\right)^{-p},$$

$$S_{21} = \frac{S_{021}}{n}\left(\frac{r}{b}\right)^{-p},\ S_{22} = \frac{S_{022}}{n}\left(\frac{r}{b}\right)^{-p},\ S_{23} = \frac{S_{023}}{n}\left(\frac{r}{b}\right)^{-p},$$

where: $a \le r \le b$; S_{011}, S_{012}, S_{013}, S_{021}, S_{022}, S_{023}, S_{031}, S_{032} and S_{033} are material constants; and $p \le 0$ is a non-homogeneity parameter.

Using these non-homogeneous material constants in Eq.(3), we get

$$\begin{aligned} T_{rr} &= \frac{S_{011}}{n}\left(\frac{r}{b}\right)^{-p}[1-(r\beta'+\beta)^n]+\frac{S_{012}}{n}\left(\frac{r}{b}\right)^{-p}[1-\beta^n]+\frac{S_{013}}{n}\left(\frac{r}{b}\right)^{-p}[1-(1-\alpha)^n],\\ T_{\theta\theta} &= \frac{S_{021}}{n}\left(\frac{r}{b}\right)^{-p}[1-(r\beta'+\beta)^n]+\frac{S_{022}}{n}\left(\frac{r}{b}\right)^{-p}[1-\beta^n]+\frac{S_{023}}{n}\left(\frac{r}{b}\right)^{-p}[1-(1-\alpha)^n],\\ T_{zz} &= 0. \end{aligned} \tag{4}$$

Equation of equilibrium is given by

$$\frac{d}{dr}(hrT_{rr}) - hT_{\theta\theta} + h\rho\omega^2 r^2 = 0, \tag{5}$$

where: thickness and density of the disk vary in the form of $h = h_0\left(\frac{r}{b}\right)^{-m}$, $\rho = \rho_0\left(\frac{r}{b}\right)^{-t}$, respectively; and angular speed of rotating disk is denoted by ω.

MATHEMATICAL FORMULATION OF THE PROBLEM

Substitution of Eq.(4) in Eq.(5) gives the following integro-differential equation

$$Br^{-m-p+1} + \int r^{-m-p}\left[S_{021}(r\beta'+\beta)^n + S_{022}\beta^n\right]dr + \frac{n\rho_0\omega^2 b^{t-p} r^{-m-t+3}}{(-m-t+3)} - r^{-m-p+1}\left[S_{011}(r\beta'+\beta)^n + S_{012}\beta^n\right] = C, \tag{6}$$

where: $B = S_{011}+S_{012}+S_{013}(1-(1-\alpha)^n) - \dfrac{S_{021}+S_{022}+S_{023}(1-(1-\alpha)^n)}{(-m-p+1)}$; and C is the constant of integration.

Substituting $r = 1/z$, and differentiating with respect to z, then Eq.(6) becomes

$$D_1 - D_2(\beta - z\beta')^n - D_3\beta^n - n\rho_0\omega^2 b^{t-p} z^{-2} + z^2 nC_{011}(\beta - z\beta')^{n-1}\beta'' - znS_{012}\beta^{n-1}\beta' = 0, \quad (7)$$

where: $D_1 = B(m + p - 1)$; $D_2 = (m + p - 1)S_{011} + S_{021}$; $D_3 = (m + p - 1)S_{012} + S_{022}$.

Substitution of $z = e^t$ and $\beta = le^{t/2}$ in Eq.(7) yields,

$$D_1 e^{-nt/2} - D_2\left(\frac{l}{2} - l'\right)^n + nC_{011}\left(\frac{l}{2} - l'\right)^{n-1}\left(l'' - \frac{l}{4}\right) - nC_{012}l^{n-1}\left(\frac{l}{2} - l'\right) - D_3 l^n - n\rho_0\omega^2 b^{t-p} e^{-\left(\frac{n+4}{2}\right)t} = 0, \quad (8)$$

where: $l' = dl/dt$.

Equation (8) on further substitution $\left(\frac{l}{2} + l'\right) = q$ gives the following ordinary nonlinear differential equation

$$\left[\left(-2D_1 e^{-nt/2} + 2n\rho_0\omega^2 b^{t-p} e^{-\left(\frac{n+4}{2}\right)t}\right) l^{-n} + 2D_3 + 2D_2\left(1 - \frac{q}{l}\right)^n + 2nS_{012}\frac{q}{l} + nS_{011}\frac{q}{l}\left(1 - \frac{q}{l}\right)^{n-1}\right]\frac{dl}{dq} = 2nS_{011}\left(1 - \frac{q}{l}\right)^{n-1}\left(\frac{q}{l} - \frac{1}{2}\right). \quad (9)$$

By substituting $q/l = F$, $1/l = Q$, Eq.(9) becomes

$$\frac{dQ}{dF} = \frac{2nS_{011}Q(1-F)^{n-1}\left(F - \frac{1}{2}\right)}{2nS_{011}F(1-F)^{n-1}\left(F - \frac{1}{2}\right) + \left(2D_1 e^{-nt/2} - 2n\rho_0\omega^2 b^{t-p} e^{-(n+4)t/2}\right)Q^n - 2D_2(1-F)^n - nS_{011}F(1-F)^{n-1} - 2nS_{012}F - 2D_3}. \quad (10)$$

The above equation has three transition points which are $F \to \pm\infty$ and $F \to 1$.

The boundary conditions are given by

$$T_{rr} = 0 \quad \text{at} \quad r = a \quad (11a)$$

and

$$T_{rr} = 0 \quad \text{at} \quad r = b. \quad (11b)$$

MATHEMATICAL SOLUTION THROUGH PRINCIPAL STRESS

For the transitional stresses and angular speed to be obtained at the transition point $F \to \pm\infty$, we need to assume a valid transition function /24-25/. The transition function R defined in terms of T_{rr} is as follows

$$R = 1 - \frac{nT_{rr}}{\left(\frac{r}{b}\right)^{-p}[S_{011} + S_{012} + S_{013}]} - \frac{n\rho\omega^2 r^2}{2\left(\frac{r}{b}\right)^{-p}[S_{011} + S_{012} + S_{013}]}. \quad (12)$$

Logarithmic differentiation of Eq.(12) with respect to r gives

$$R = M r^{(m+p-1)+N}, \quad (13)$$

where: $N = S_{021}/S_{011}$ and M is the constant of integration.

Comparing Eqs.(12) and (13), we get

$$T_{rr} = \left(\frac{r}{b}\right)^{-p}\frac{J}{n} - \frac{M r^{m-1+N} J}{nb^{-p}} - \frac{\rho_0\omega^2 r^{-t+2}}{2b^{-t}}, \quad (14)$$

where: $J = S_{011} + S_{012} + S_{013}$.

Using Eq.(11a) in Eq.(14), we get

$$M = a^{-m-p+1-N} - \frac{n\rho_0\omega^2 b^{t-p} a^{-t-m+3-N}}{2J}. \quad (15)$$

Using Eq.(11b) and Eq.(15) in Eq.(14), we get

$$\rho_0\omega^2 a^2 = \frac{2J}{n}\left(\frac{a}{b}\right)^2 \cdot \frac{1 - \left(\frac{a}{b}\right)^{-p-m+1-N}}{1 - \left(\frac{a}{b}\right)^{-m-t+3-N}} \quad (16)$$

Stresses and angular speed at initial yielding are

$$T_{rr} = \frac{J}{n}\left[\left(\frac{r}{b}\right)^{-p} - \left(\frac{r}{a}\right)^{m-1+N}\left(\frac{a}{b}\right)^{-p}\right] + \frac{\rho_0\omega^2 a^2}{2}\left[\left(\frac{r}{a}\right)^{m-1+N}\left(\frac{a}{b}\right)^{-t} - \left(\frac{r}{b}\right)^{-t+2}\left(\frac{a}{b}\right)^{-2}\right], \quad (17)$$

$$T_{\theta\theta} = \frac{J}{n}\left[(-m-p+1)\left(\frac{r}{b}\right)^{-p} - N\left(\frac{r}{a}\right)^{m-1+N}\left(\frac{a}{b}\right)^{-p}\right] + \frac{\rho_0\omega^2 a^2}{2}\left[N\left(\frac{r}{a}\right)^{m-1+N}\left(\frac{a}{b}\right)^{-t} - (-t-m+1)\left(\frac{r}{b}\right)^{-t}\left(\frac{r}{a}\right)^2\right], \quad (18)$$

and

$$\omega^2 = \frac{2J}{n\rho_0 b^2} \cdot \frac{1 - \left(\frac{a}{b}\right)^{-p-m+1-N}}{1 - \left(\frac{a}{b}\right)^{-m-t+3-N}}. \quad (19)$$

The material constants for fully plastic state /23/ are as: $S_{011} = S_{012} = S_{013}$, $S_{021} = S_{022} = S_{023}$.

The stresses and angular speed at fully plastic state are

$$T_{rr} = \frac{3S_{011}}{n}\left[\left(\frac{r}{b}\right)^{-p} - \left(\frac{r}{a}\right)^{m-1+N}\left(\frac{a}{b}\right)^{-p}\right] + \frac{\rho_0\omega^2 a^2}{2}\left[\left(\frac{r}{a}\right)^{m-1+N}\left(\frac{a}{b}\right)^{-t} - \left(\frac{r}{b}\right)^{-t}\left(\frac{r}{a}\right)^2\right], \quad (20)$$

$$T_{\theta\theta}=\frac{3S_{011}}{n}\left[(-m-p+1)\left(\frac{r}{b}\right)^{-p}-N\left(\frac{r}{a}\right)^{m-1+N}\left(\frac{a}{b}\right)^{-p}\right]+\frac{\rho_0\omega^2a^2}{2}\left[N\left(\frac{r}{a}\right)^{m-1+N}\left(\frac{a}{b}\right)^{-t}-(-t-m+1)\left(\frac{r}{b}\right)^{-t}\left(\frac{r}{a}\right)^{2}\right], \quad (21)$$

and

$$\omega^2=\frac{6S_{011}}{n\rho_0b^2}\cdot\frac{1-\left(\frac{a}{b}\right)^{-p-m+1-N}}{1-\left(\frac{a}{b}\right)^{-t-m+3-N}}. \quad (22)$$

The dimensional quantities converted into non-dimensional quantities are as

$$R=\frac{r}{b},\ R_0=\frac{a}{b},\ \sigma_{rr}=\frac{T_{rr}}{Y},\ \sigma_{\theta\theta}=\frac{T_{\theta\theta}}{Y},\ \Omega_i^2=\frac{\rho_0\omega^2a^2}{Y_i},\ \Omega_f^2=\frac{\rho_0\omega^2b^2}{Y_f},\ J_1=\frac{J}{Y_i},$$

where: Y_i and Y_f are yield stresses at initial and fully plastic state, respectively.

For initial yielding, transitional stresses and angular speed in non-dimensional form are given as

$$\sigma_{rr}=\frac{J_1}{n}\left[R^{-p}-\left(\frac{R}{R_0}\right)^{m-1+N}R_0^{-p}\right]+\frac{\Omega_i^2}{2}\left[\left(\frac{R}{R_0}\right)^{m-1+N}R_0^{-t}-\left(\frac{R}{R_0}\right)^{2}R^{-t}\right], \quad (23)$$

$$\sigma_{\theta\theta}=\frac{J_1}{n}\left[(-m-p+1)R^{-p}-N\left(\frac{R}{R_0}\right)^{m-1+N}R_0^{-p}\right]+\frac{\Omega_i^2}{2}\left[N\left(\frac{R}{R_0}\right)^{m-1+N}R_0^{-t}-(-m-t+1)\left(\frac{R}{R_0}\right)^{2}R^{-t}\right], \quad (24)$$

and

$$\Omega_i^2=\frac{2J_1R_0^2}{n}\cdot\frac{1-R_0^{-p-m+1-N}}{1-R_0^{-m-t+3-N}}. \quad (25)$$

For fully plastic state /23/, $S_{011}=S_{012}=S_{013}$, $S_{021}=S_{022}=S_{023}$.

For full plasticity, transitional stresses and angular speed in non-dimensional form are given as

$$\sigma_{rr}=\frac{3S_{011}}{nY_f}\left[R^{-p}-\left(\frac{R}{R_0}\right)^{m-1+N}R_0^{-p}\right]+\frac{\Omega_f^2R_0^2}{2}\left[\left(\frac{R}{R_0}\right)^{m-1+N}R_0^{-t}-\left(\frac{R}{R_0}\right)^{2}R^{-t}\right], \quad (26)$$

$$\sigma_{\theta\theta}=\frac{3S_{011}}{nY_f}\left[(-m-p+1)R^{-p}-N\left(\frac{R}{R_0}\right)^{m-1+N}R_0^{-p}\right]+\frac{\Omega_f^2R_0^2}{2}\left[N\left(\frac{R}{R_0}\right)^{m-1+N}R_0^{-t}-(-m-t+1)\left(\frac{R}{R_0}\right)^{2}R^{-t}\right], \quad (27)$$

and

$$\Omega_f^2=\frac{6S_{011}}{nY_f}\cdot\frac{1-R_0^{-p-m+1-N}}{1-R_0^{-m-t+3-N}}. \quad (28)$$

NUMERICAL ILLUSTRATION AND DISCUSSION

Mathematica software has been used to evaluate numerical values of angular speed and circumferential stresses for initial yielding and full plasticity by taking thickness and density parameters as m = 0.2 and t = 1.1 in Eqs.(24), (25), (27) and (28). Radii ratio against angular speed required for initial yielding and full plasticity with varying nonlinearity and nonhomogeneity parameters for different materials can be seen from Figs. 1-6. Figures 7-12 show radii ratio against circumferential stresses required for initial yielding and full plastic state with varying nonlinearity and nonhomogeneity parameters for different materials.

It has been noticed from Table 2 for functionally graded rotating disk that angular speed decreases with increase in nonhomogeneity of the material, while angular speed increases with increase in radii ratio. Also, the percentage increase in angular speed required for initial yielding to become fully plastic is high for the rotating disk with radii ratio 0.3.

Using data from Table 1, we obtained angular speeds as plotted in Figs. 1-6, for p = -1, -2, -3, -4, -5 against radii ratio R_0.

Figure 1 shows that for disk made of functionally graded material having variable thickness and density with linear measure, angular speed required for initial yielding is maximal at the external surface. It has also been observed that angular speed required for initial yielding is on the higher side for the disk made up of non-homogeneity parameter p = -5, as compared to disk with other non-homogeneity parameters. It has also been observed that for linear measure, the angular speed required for initial yielding is higher for functionally graded barite as compared to the functionally graded topaz and steel. A significant change has been observed in angular speed required for initial yielding in a rotating disk when the measure has been changed from linear to nonlinear, as can be seen from Fig. 2. With the increase in nonlinearity of the measure, the angular speed required for initial yielding further increases which can be seen in Fig. 3.

It has been noticed from Table 2 for functionally graded rotating disk that angular speed decreases with the increase in non-homogeneity of the material, while angular speed increases with the increase in radii ratio. Also, percentage increase in angular speed required for initial yielding to become fully plasticity is high for rotating disk with radii ratio 0.3.

Table 1. Values of material constants for different materials (in units of 10^{11} N/m^2).

Materials	S_{011}	S_{012}	S_{013}	S_{021}	S_{022}	S_{023}
Barite (orthotropic material)	0.8941	0.4614	0.2691	0.4614	0.7842	0.2676
Topaz (orthotropic material)	2.8145	1.2552	0.8433	1.2552	3.4911	0.8825
Steel (isotropic material)	5.326	3.688	3.688	3.688	5.326	3.688

Table 2. Angular speed against radii ratios for functionally graded disk having variable thickness and density.

m = 0.4, t = 1.2, n = 1/3		Angular speed			Percentage increase in angular speed required from initial yielding to fully plastic state		
		R_0 = 0.3	R_0 = 0.5	R_0 = 0.7	R_0 = 0.3	R_0 = 0.5	R_0 = 0.7
Functionally graded steel							
p = -1	Ω_i^2	2.15596	6.22267	12.5544	211.099456	86.65957304	33.327857
	Ω_f^2	20.866	21.6809	22.3171			
p = -3	Ω_i^2	3.14573	11.5512	29.3052	211.099056	86.65944402	33.3283
	Ω_f^2	30.4452	40.2464	52.0942			
p = -5	Ω_i^2	3.23481	12.8833	37.5132	211.099356	86.65950794	33.328202
	Ω_f^2	31.3074	44.8877	66.685			
Functionally graded barite							
p = -1	Ω_i^2	3.62751	10.4423	21.0463	134.9758	40.94621	0.703823085
	Ω_f^2	20.0288	20.7445	21.3436			
p = -3	Ω_i^2	4.85563	17.436	43.7873	134.9758	40.84268	0.703891879
	Ω_f^2	26.8097	34.5872	44.4059			
p = -5	Ω_i^2	4.96616	19.1844	54.9304	134.9759	40.82854	0.703871224
	Ω_f^2	27.42	38.0478	55.7064			
Functionally graded topaz							
p = -1	Ω_i^2	3.45857	9.94737	20.0376	139.1977	43.5078	2.51338
	Ω_f^2	19.7884	20.4861	21.0575			
p = -3	Ω_i^2	4.50332	16.036	40.1048	139.1982	43.50753	2.513615
	Ω_f^2	25.7661	33.0252	42.1463			
p = -5	Ω_i^2	4.59735	17.5581	49.9377	139.1982	43.50778	2.513679
	Ω_f^2	26.3041	36.16	52.4798			

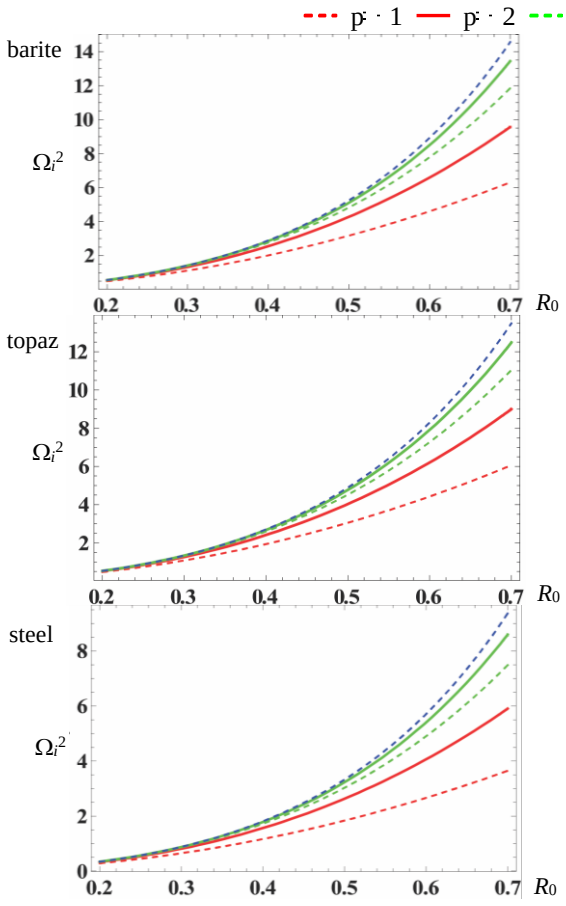

Figure 1. Angular speed required for initial yielding for functionally graded rotating disk with linear measure.

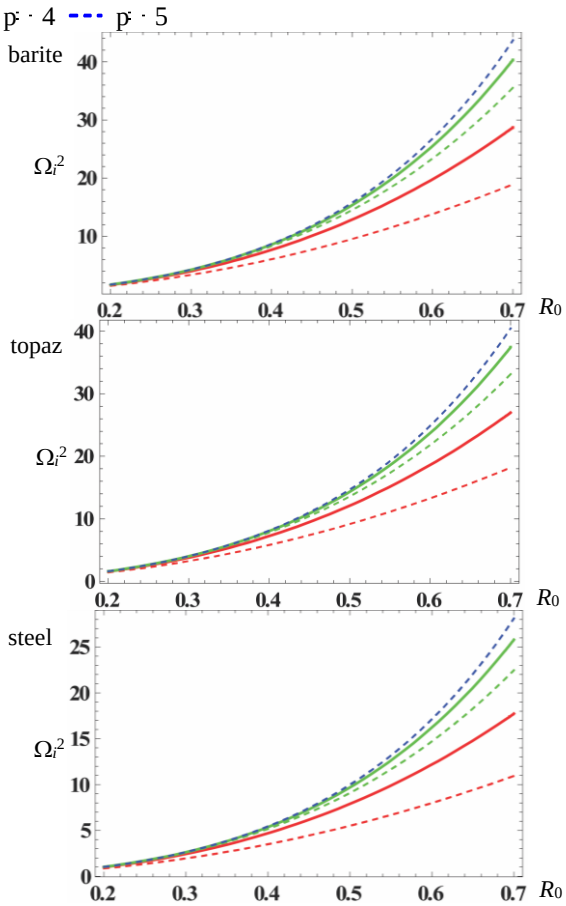

Figure 2. Angular speed required for initial yielding for functionally graded rotating disk with nonlinear measure n = 1/3.

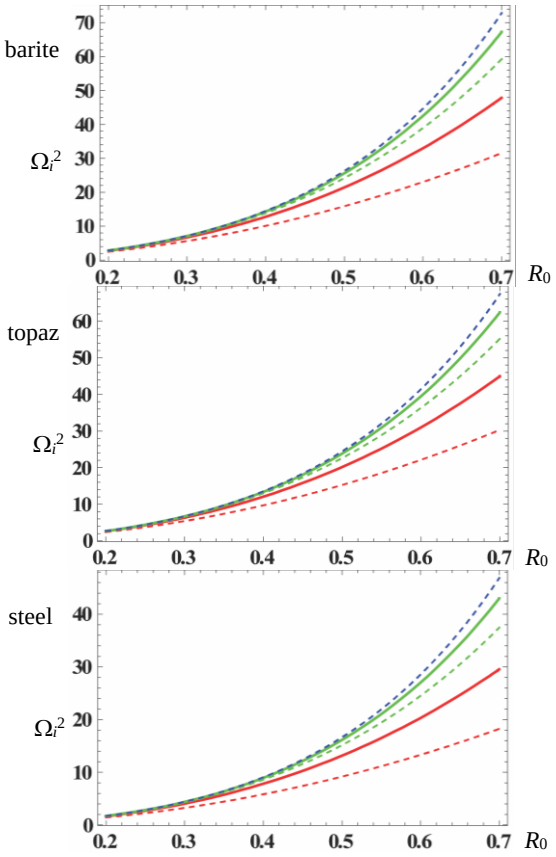

Figure 3. Angular speed required for initial yielding for functionally graded rotating disk with nonlinear measure n = 1/5.

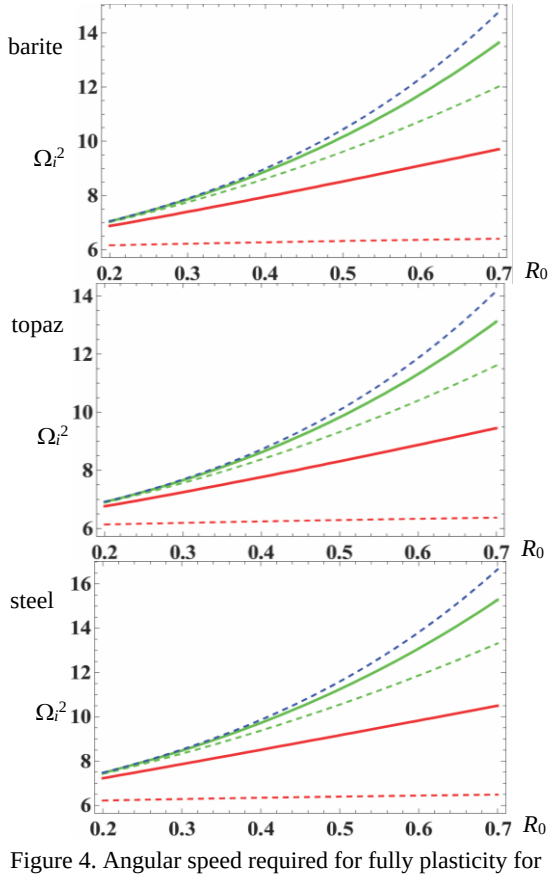

Figure 4. Angular speed required for fully plasticity for functionally graded rotating disk for linear measure.

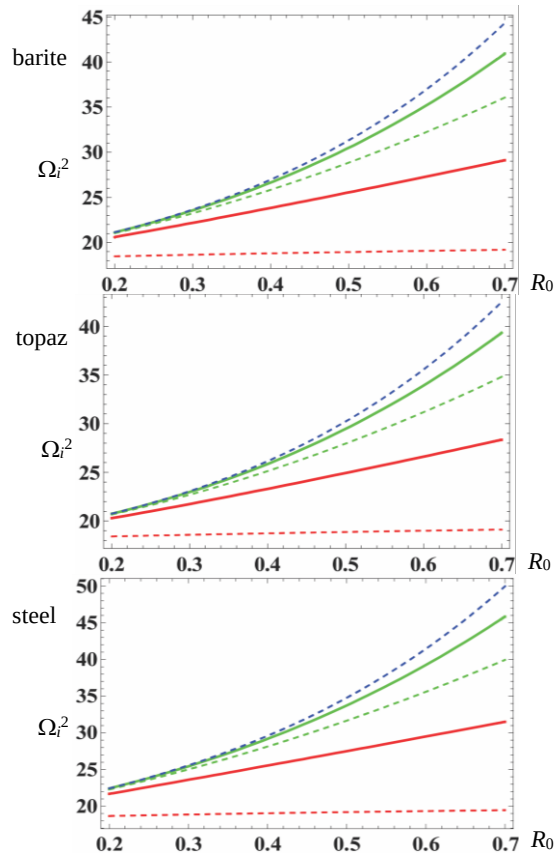

Figure 5. Angular speed required for fully plasticity for functionally graded rotating disk with nonlinear measure n = 1/3.

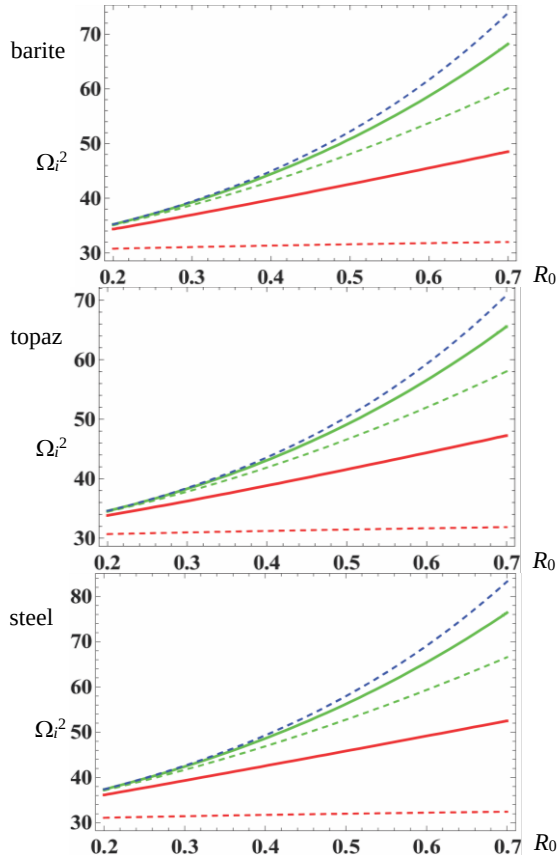

Figure 6. Angular speed required for fully plasticity for functionally graded rotating disk with nonlinear measure n = 1/5.

From Fig. 4 we have noticed that angular speed required for fully plastic state for a functionally graded disk with linear measure is higher at external surface with non-homogeneity parameter p = -5 as compared to disk with other non-homogeneity parameters. It has also been noticed that functionally graded steel has higher angular speed as compared to that of topaz and barite for linear measure. A significant change in angular speed has been observed when the measure changes from linear to nonlinear as can be seen in Fig. 5. It can be analysed from Fig. 6 that as the nonlinearity of the functionally graded rotating disk increases, the required angular speed increases simultaneously.

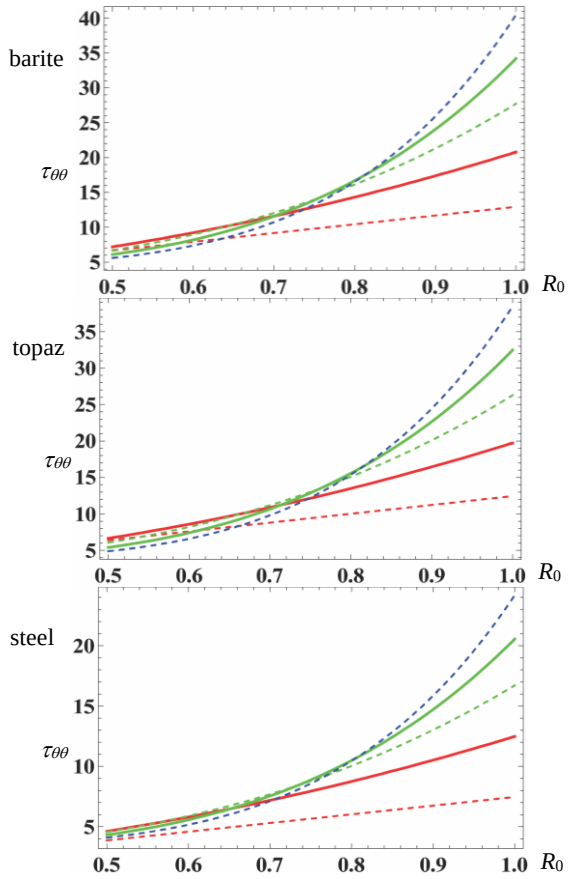

Figure 7. Circumferential stress required for initial yielding for functionally graded rotating disk with linear measure.

It has been observed from Fig. 7 that thin rotating functionally graded disk with variable thickness and density shows maximum circumferential stresses at the external surface. It has also been noticed that the non-homogeneity parameter p = -5 gives higher circumferential stresses on the external surface of the disk as compared to other non-homogeneity parameters. It has also been noticed that for linear measure the circumferential stresses are higher for functionally graded barite than functionally graded topaz and steel. As the measure changes from linear to nonlinear, a significant change has been noticed in circumferential stresses for the rotating disk which can be seen in Fig. 8. These circumferential stresses further increase with the increase in nonlinearity measure (Fig. 9).

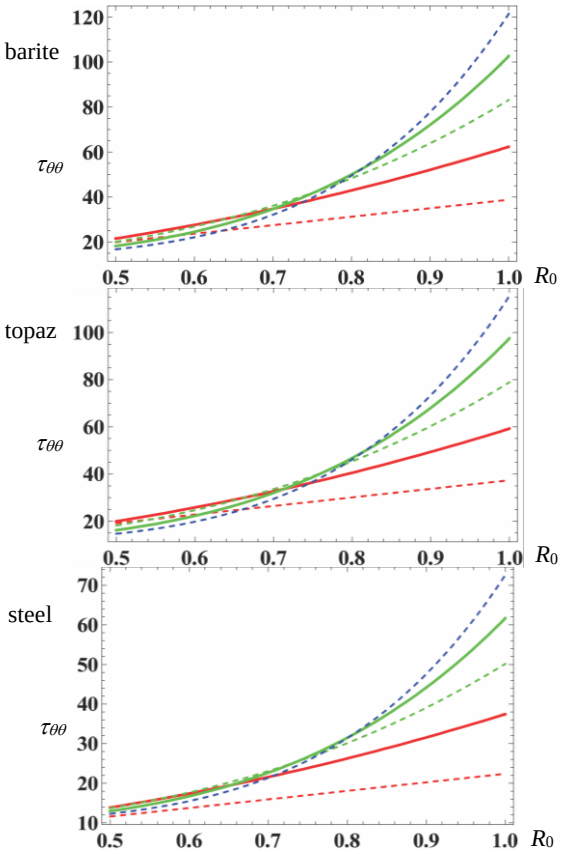

Figure 8. Circumferential stress required for initial yielding for functionally graded rotating with nonlinear measure n = 1/3.

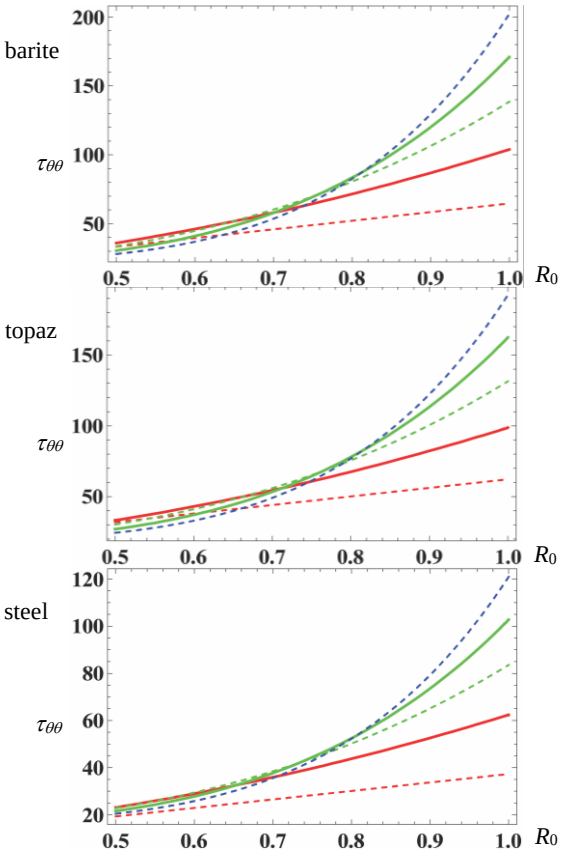

Figure 9. Circumferential stress required for initial yielding for functionally graded rotating disk with nonlinear measure n = 1/5.

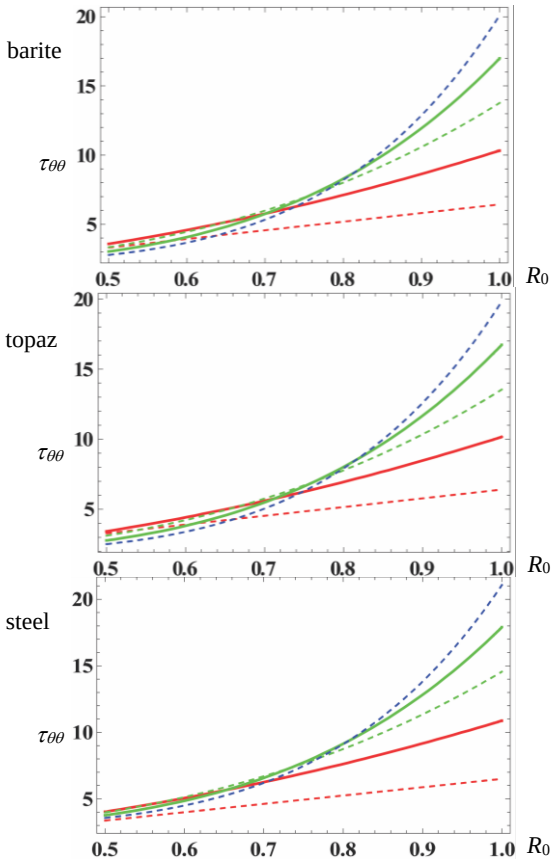

Figure 10. Circumferential stress required for fully plasticity for functionally graded rotating with linear measure.

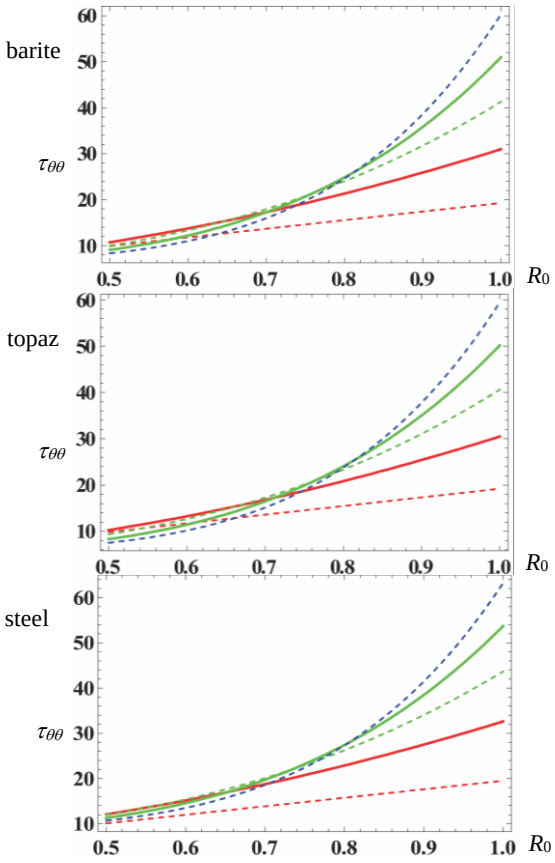

Figure 11. Circumferential stress required for fully plasticity for functionally graded rotating with nonlinear measure n = 1/3.

It has been analysed from Fig. 10 that circumferential stresses for fully plastic state with linear measure are higher at external surface for a disk made up of functionally graded material with variable thickness and density. It has also been noticed that as the non-homogeneity of the disk increases, the circumferential stresses required for fully plastic state increases. Also, circumferential stresses obtained for functionally graded steel are higher than functionally graded topaz and barite.

Circumferential stresses required for fully plastic state in a rotating disk have a significant change, when the measure changes from linear to nonlinear, as can be seen in Fig. 11. Figure 12 shows that the increase in fully plastic circumferential stresses is due to the increase in nonlinearity of the measure.

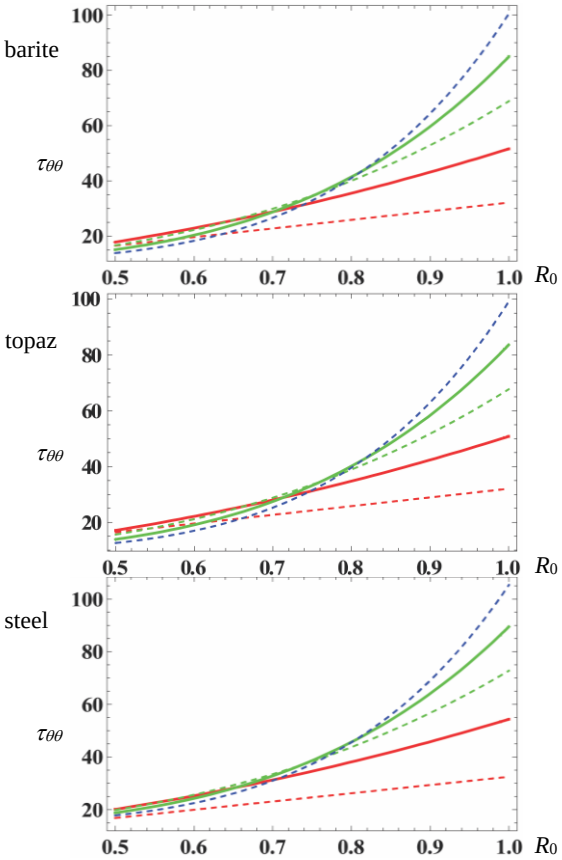

Figure 12. Circumferential stress required for fully plasticity for functionally graded rotating with nonlinear n = 1/5.

CONCLUSION

From the above numerical discussion, it is concluded that percentage increase in angular speed required from initial yielding to fully plastic state is high for functionally graded steel as compared to functionally graded barite and topaz while this percentage increase is higher for functionally graded topaz as compared to functionally graded barite. Also, from the discussion of circumferential stresses it has been concluded that circumferential stresses are less for functionally graded steel as compared to functionally graded barite and topaz.

Thus, functionally graded steel is best suitable for engineering design as compared to functionally graded ortho-

tropic materials while topaz is better choice of designing as compared to functionally graded barite.

REFERENCES

1. Timoshenko S.P., Goodier J.N., Theory of Elasticity, 3rd Ed., McGraw-Hill, New York, 1970.
2. Sadd, M.H., Elasticity: Theory, Applications and Numerics, Academic Press, Elsevier, 2005.
3. Chakrabarty, J., Theory of Plasticity, 3rd Ed., Elsevier Butterworth-Heinemann, San Diego, 2006.
4. Suresh, S., Mortensen A., Fundamentals of Functionally Graded Materials, IOM3, Maney Publishing, London, UK, 1998.
5. Eraslan, A.N., Akgül, F. (2005), *Yielding and elastoplastic deformation of annular disks of a parabolic section subject to external compression*, Turk. J Eng. Environ. Sci. 29(1): 51-60.
6. You, L.H., Tang, Y.Y., Zhang, J.J., Zheng C.Y. (2000), *Numerical analysis of elastic-plastic rotating disks with arbitrary variable thickness and density*, Int. J Solids Struct. 37(52): 7809-7820. doi: 10.1016/S0020-7683(99)00308-X
7. Radaković, Z., Lenkey, Gy.B., Grabulov, V., Sedmak, A. (1999), *Application of two independent measurement techniques for determination of ductile crack growth initiation*, Int. J Fracture, 96(2): 23-28.
8. Sharma, S., Yadav, S. (2019), *Numerical solution of thermal elastic-plastic functionally graded thin rotating disk with exponentially variable thickness and variable density*, Thermal Sci., 23(1): 125-136. doi: 10.2298/TSCI131001136S
9. Bayat, M., Saleem, M., Sahari, B.B., et al. (2008), *Analysis of functionally graded rotating disks with variable* thickness, Mechanics Research Communications, 35(5): 283-309. doi: 10.1016/j.mechrescom.2008.02.007
10. Zheng, Y., Bahaloo, H., Mousanezhad, D., et al. (2016), *Stress analysis in functionally graded rotating disks with non-uniform thickness and variable angular velocity*, Int. J Mech. Sci. 119: 283-293. doi: 10.1016/j.ijmecsci.2016.10.018
11. Dai, T., Dai, H-L. (2017), *Analysis of a rotating FGMEE circular disk with variable thickness under thermal environment*, Appl. Math. Model. 45: 900-924. doi: 10.1016/j.apm.2017.01.007
12. Bayat, M., Sahari, B.B., Saleem, M., et al. (2009), *Thermoelastic solution of a functionally graded variable thickness rotating disk with bending based on the first-order shear deformation theory*, Thin-Walled Struc. 47(5): 568-582. doi: 10.1016/j.tws.2008.10.002
13. Bahaloo, H., Papadopolus, J., Ghosh, R., et al. (2016), *Transverse vibration and stability of a functionally graded rotating annular disk with a circumferential crack*, Int. J Mech. Sci. 113: 26-35. doi: 10.1016/j.ijrnecsci.2016.03.004
14. Asghari, M., Ghafoori, E. (2010), *A three-dimensional elasticity solution for functionally graded rotating disks*, Compos. Struct. 92(5): 1092-1099. doi: 10.1016/j.compstruct.2009.09.055
15. Bayat, M., Saleem, M., Sahari B. B., et al. (2009), *Mechanical and thermal stresses in a functionally graded rotating disk with variable thickness due to radially symmetry loads*, Int. J Pres. Ves. Piping, 86: 357-372. doi: 10.1016/j.ijpvp.2008.12.006
16. Çallıoğlu, H., Sayer, M., Demir, E. (2015), *Elatic-plastic stress analysis of rotating functionally graded discs*, Thin-Walled Struct. 94: 38-44. doi: 10.1016/j.tws.2015.03.016
17. Dai, T., Dai, H-L. (2016), *Thermo-elastic analysis of functionally graded rotating hollow circular disk with variable thickness and angular speed*, Appl. Math. Model. 40(17-18): 7689-7707. doi: 10.1016/j.apm.2016.03.025
18. Zafarmand, H., Kadkhodayan, M. (2015), *Non-linear analysis of functionally graded nanocomposite rotating disks with variable thickness reinforced with carbon nanotubes*, Aerosp. Sci. Techn. 41: 47-54. doi: 10.1016/j.ast.2014.12.002
19. Bose, T., Rattan, M. (2018), *Effect of thermal gradation on steady state creep of functionally graded rotating disc*, Europ. J Mech.-A/Solids, 67: 169-176. doi: 10.1016/j.euromechsol.2017.09.014
20. Borah B.N. (2005), *Thermo-elastic-plastic transition*, Contemp. Math. 379: 93-111. doi: 10.1090/conm/379/07027
21. Sharma, S., Sahai, I., Kumar, R. (2014), *Thermo elastic-plastic transition of transversely isotropic thick-walled circular cylinder under internal and external pressure*, Multidisc. Model. Mater. Struct. 10(2): 211-227. doi: 10.1108/MMMS-03-2013-0026
22. Sharma, S. (2017), *Stress analysis of elastic-plastic thick-walled cylindrical pressure vessels subjected to temperature*, Struct. Integ. and Life, 17(2): 105-112.
23. Sharma, S., Panchal, R. (2018), *Elastic-plastic transition of pressurized functionally graded orthotropic cylinder using Seth's transition theory*, J Solid Mech. 10(2): 450-463.
24. Sharma, S., Maheshwari, K. (2019), *Creep stresses in functionally graded thin rotating orthotropic disk with variable thickness and density*, AIP Conf. Proc. 2061(1): 020036-1-7. doi: 10.1063/1.5086658
25. Sharma, S. (2017), *Creep transition in bending of functionally graded transversely isotropic rectangular plates*, Struct. Integ. and Life, 17(3): 187-192.